A DUAL FUNCTION PARYLENE-BASED BIOMIMETIC TACTILE SENSOR AND ACTUATOR FOR NEXT GENERATION MECHANICALLY RESPONSIVE MICROELECTRODE ARRAYS

C.A. Gutierrez and E. Meng*
University of Southern California, Los Angeles, California, USA

ABSTRACT

We present the first multimodal Parylene-based biomimetic platform with the ability to measure tactile forces while simultaneously enabling active stimulation/recording of neural tissue via movable microelectrodes. A liquid-filled microchamber encapsulating interdigitated microelectrodes performs the *dual functions* of actuation and tactile sensing. The electrodes are impedance-based tactile sensing elements and sites for electrolytic gas generation for pneumatic control of microelectrode position. Impedance sensitivity of up to 1.7 %/μm and out-of-plane positioning up to 8 μm were demonstrated. We also report on the mechanotransduction of biomimetic channel structures.

KEYWORDS

Parylene C, Tactile sensing, Movable electrodes.

INTRODUCTION

Most neural prostheses function by recording and/or stimulating tissue via microelectrodes. Some notable examples include cortical prosthesis [1] and retinal prosthesis [2, 3] efforts which employ microelectode arrays (MEAs) to restore function by selective electrical stimulation of the surrounding tissues.

Traditionally, MEAs have been electrode-only and research efforts primarily focus on flexibility for conformal application, high density electrodes, and implantability. These characteristics can be addressed by using polymers such as Parylene as the structural material. Parylene is used for its United States Pharmacopoeia (USP) Class VI biocompatibility, mechanical strength (~4GPa), MEMS compatibility and flexibility which enables released MEAs to conform to three-dimensional tissue surfaces unlike MEAs bound to rigid substrates. Although these considerations offer great improvements, the efficacy of electronic neural prostheses, such as the intraocular retinal prosthesis, is ultimately dependent on the electromechanical coupling between the device and tissue [3]. Factors such as proximity, temperature, pressure, and post-implantation micromotion all impact the overall function of a neural prosthesis. These factors cannot be adequately addressed using current electrode-only technologies.

Here we present an enabling technology for next generation multimodal MEAs. This dual function device is capable of providing key tactile information at the tissue/device interface and has the ability to respond mechanically by adjusting the out-of-plane electrode position. We also show biomimetic operation via axon-like tactile sensing structures. The quantification of mechanically induced strains at the tissue-prosthesis interface will provide additional understanding of the biological and electrophysiological effects of neural prosthetic implants.

DEVICE DESIGN

The key elements of this platform design are a liquid-filled chamber encapsulating interdigitated electrodes and a self-sealing stiction valve. The device has two possible configurations: (1) a tactile sensor and (2) a movable electrode actuator (Figure 1a, b). Liquid encapsulation is accomplished by immersing the device in a liquid which then fills a chamber through the stiction valve port. The device is then exposed to air where the evaporative drying process will cause the valve to collapse due to stiction, thereby sealing the remaining liquid in the chamber.

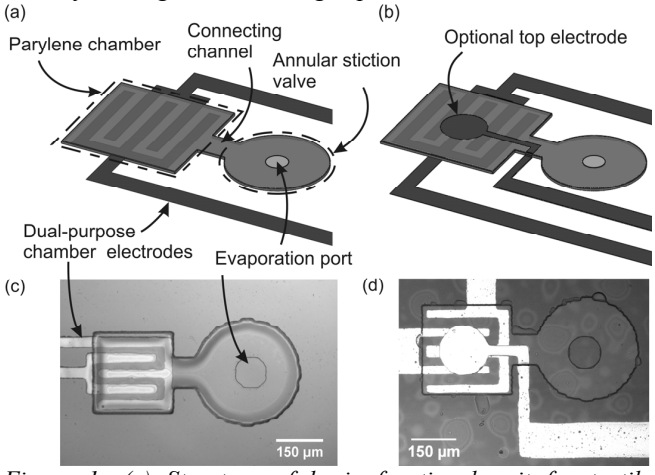

Figure 1: (a) Structure of basic functional unit for tactile sensing. Stiction valve enables liquid encapsulation in Parylene chamber. (b) Movable electrode configuration; optional top electrode is pneumatically actuated as chamber membrane deflects upward. (c)-(d) Single fabricated devices.

Operating principles

The dual modes of operation are depicted in Figure 2. Tactile sensing utilizes the electrochemical impedance of the encapsulated liquid and is dependent on liquid volume and ionic conduction path between the two electrodes (Figure 2a). Under tactile deformation, the volumetric conduction path within the chamber is altered, analogous to a variable resistance. This phenomenon enables measurement of the tactile force acting on the chamber

membrane.

Out-of-plane actuation of the top electrode is accomplished by applying a constant current (~5 μA for a few seconds) across the chamber electrodes to initiate electrolysis. The evolution of hydrogen and oxygen gas within the chamber generates an internal pressure causing the electrode to deflect upward (Figure 2b).

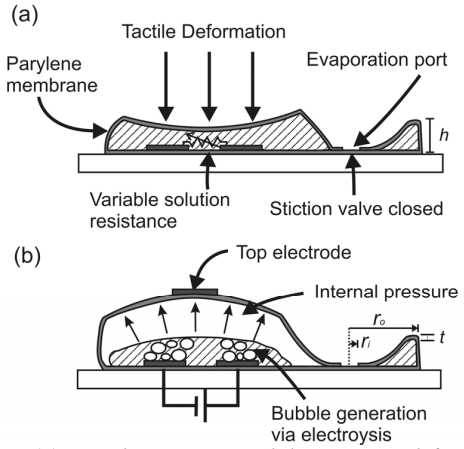

Figure 2: (a) Tactile sensing modality. External forces deform chamber altering liquid conductive path between bottom electrodes. (b) Movable electrode modality. Increased chamber pressure from electrolytic gas generation pneumatically actuates top electrode.

Stiction valve

The design guidelines for annular stiction valves were previously investigated in [4, 5]. Stiction occurs for critical number $N_c > 1$ where

$$N_c = \frac{\sigma r_o^{\,4}}{Dh^2} p(\phi, \upsilon) \qquad (1)$$

with $\sigma = 2\gamma_{LA}\cos\theta_C$, $D = (Et^3/12(1-\upsilon^2))$ and where γ_{LA} is the liquid-air surface tension, θ_C is the Parylene contact angle, E is Young's Modulus, t is the membrane thickness, h is the membrane height, ν is Poisson's ratio, ϕ is the ratio r_i/r_o and p is a numerical function of ϕ and υ.

DEVICE FABRICATION

A standard soda-lime wafer was optionally treated with silane A-174 Parylene adhesion promoter. Released devices did not require this step. Parylene C was deposited (~10 μm) on the entire wafer. Photoresist was then spun-on and pattered for metal lift-off forming chamber electrodes, leads, and contact pads. A sacrificial photoresist layer (10-22 μm) of AZ 4620 was patterned to define the valve and chamber structures. Parylene (2-8 μm) was then deposited followed by an optional dual-layer photoresist (AZ1518/AZ4620) lift-off process to pattern the stimulation/recording electrodes atop the chamber structures. The dual layer lift-off process with a globally exposed bottom layer was necessary to achieve continuity between substrate and the top of the chamber. The Parylene covering the contact pads and stiction valve port was etched using oxygen plasma (100 W, 100 mT). Devices were diced and soaked in acetone to remove the sacrificial photoresist. After rinsing in isopropyl alcohol and DI water, dies were immersed in an electrolyte (DI water) (Figures 3, 4).

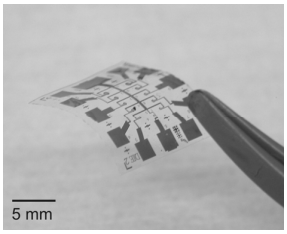

Figure 3: Released flexible array.

RESULTS AND DISCUSSION

Stiction valve

Valves (OD: 330 μm, ID: 100 μm) were fabricated and sealed within a few minutes of evaporation drying at ambient conditions (Figure 5).

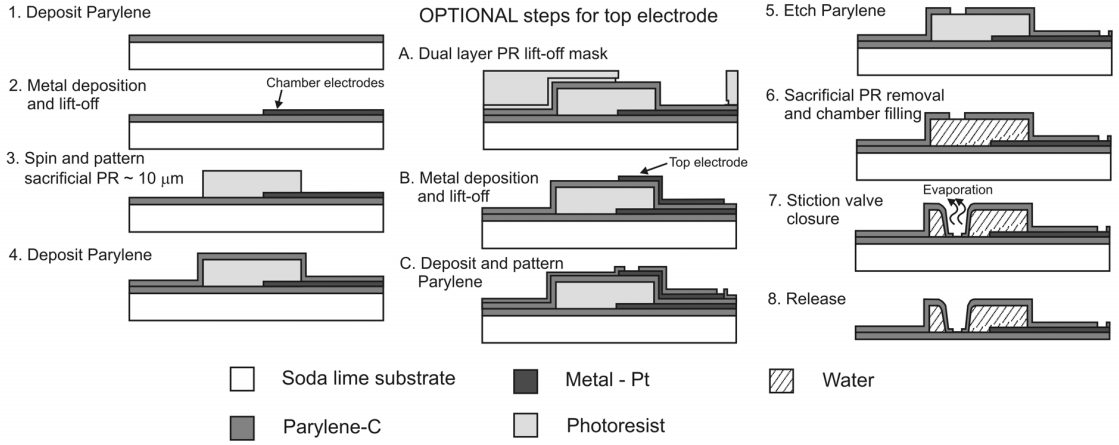

Figure 4: Fabrication process for tactile sensor/actuator platform. Steps 1-8 show tactile sensor fabrication. Steps 1-8 plus A-C (added between steps 4 and 5) show movable electrode fabrication.

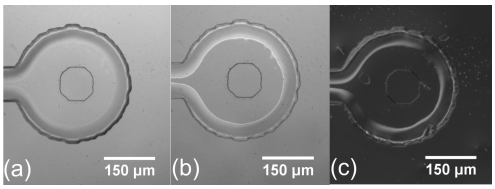

Figure 5: (a) Stiction valve open. (b) Stiction valve closed. (c) Nomarski image highlighting regions of collapse. Border fringes indicate areas where membrane has not touched down.

Experimental setup

Experiments validated the two modes of operation: impedance-based tactile sensing and actuation of electrodes. Tactile sensing was evaluated by indenting the chamber membrane with a micromanipulator stylus. Stylus displacement was measured under a 100x microscope objective with 1μm vertical resolution. The same technique was used to measure electrode displacement.

Impedance was measured using a voltage divider with active rectification to attain the DC level of the AC response (Figure 6). A LabVIEW-controlled Keithley 2400 precision multimeter was used to record the real-time impedance response. The circuit was calibrated using an Agilent E4980A precision LCR meter.

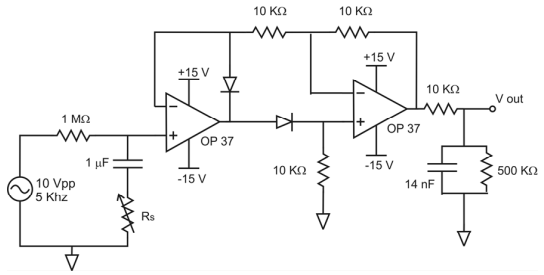

Figure 6: Impedance measurement circuit.

Tactile sensing

Impedance-indentation results for circular chambers with diameters ranging from 300 to 500 µm were obtained. Percent change in impedance per micron of indentation was greatest for 500 µm chambers with a sensitivity of 1.69 %/µm (Figure 7). Indentation depth was limited by the as-fabricated chamber height and is easily increased. This result indicates a trade-off between sensor response and size. The greater displacement of liquid volumes in larger chambers creates larger impedance responses at the cost of overall footprint.

Figure 8 shows real-time impedance based tactile detection capability. A stylus was used to indent the membrane down to the substrate several times over the full vertical travel of the suspended membrane height.

Mechanically responsive electrodes

Electrode actuation was demonstrated by applying a constant current (~5 μA for a few seconds) across the chamber electrodes and measuring deflection of the membrane surface due to electrolysis (Figure 9). On average the maximum deflection increases with larger chambers. This is due to the greater compliance of the larger membranes which allows for greater deflections.

Maximum deflections of ~8 μm were achieved with 500 μm square chambers. Corrugated membranes or bellows may extend the actuation range but electrode tethering will need to be addressed.

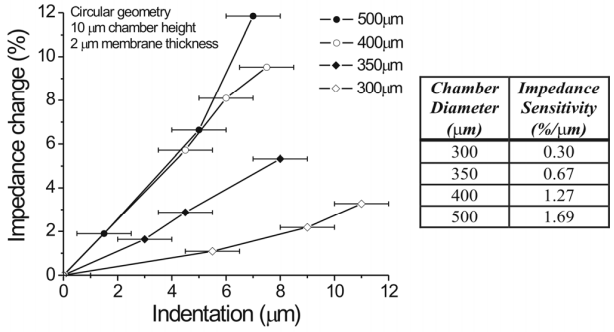

Chamber Diameter (µm)	*Impedance Sensitivity (%/µm)*
300	0.30
350	0.67
400	1.27
500	1.69

Figure 7: Percent change in solution impedance vs. membrane indentation depth for circular chamber devices. Error bars correspond to measurement resolution of microscope. Table lists the maximum impedance sensitivities obtained.

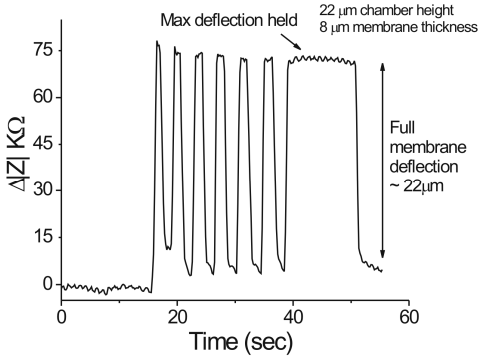

Figure 8: Real-time tactile sensor operation capturing several quick indentations followed by a sustained indentation through the full dynamic range of devices. Intermediate levels of deformation were also readily detectable.

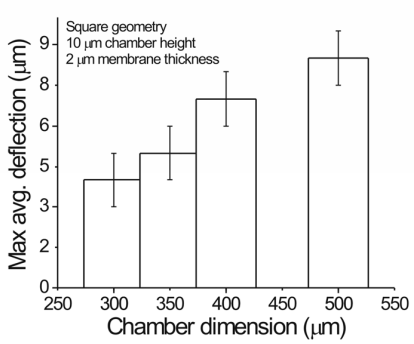

Figure 9: Electrolysis actuation. Maximum chamber deflection for square chambers. 5 μA is typically applied for about 5 seconds to achieve deflection.

Modeling

Nonlinear finite-element modeling (FEM) was used to simulate membrane tactile deformation under the stylus tip (Figure 10a). Forces of 6 mN are required for maximal deflection of 8 μm thick membranes. The force sensitivity of the device depends on chamber parameters, such as membrane thickness and chamber size [6], and can be designed to achieve a desired range. Forces acting locally on tissues at a neural prosthetic interface may range from several hundred micronewtons to a few millinewtons [7-9].

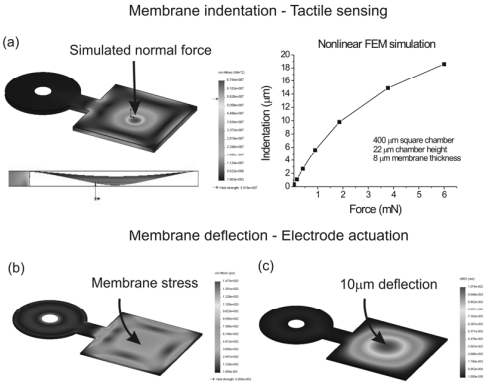

Figure 10: (a) Nonlinear FEM simulations of membrane deflection under a normally applied force to center of chamber. 6 mN required for ~18 μm membrane indentation. (b) Resultant stress distribution with 0.1 psi internal chamber pressure and (c) membrane deflection of 10 μm.

Linear modeling of membrane actuation was used to optimize routing of the top electrode leads (Figure 10b). The low stress in the connecting channel region during deflection ensures minimum membrane tethering by leads and reduces the possibility of metal fracture during deflection (Figure 11).

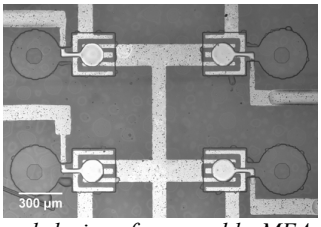

Figure 11: Arrayed devices for movable MEA. Electrode leads are optimally routed over the connecting channel.

Biomimetic tactile sensing

Fabrication of channels enables axon-like structures to mimic mechanotransduction phenomenon seen in neuronal signal propagation. Multiple electrodes can populate a channel segment allowing for downstream tactile detection. An indentation of the channel was detectable up to 1 mm away from the measurement site (Figure 12). The ability to detect tactile information along the length of a channel extends the physical sensing range of the sensor and is a modality of interest for new bio-inspired devices.

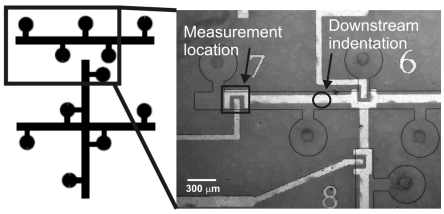

Figure 12: Axon-mimetic configuration for tactile detection.

CONCLUSION

A dual-function device for next generation MEAs was designed and fabricated. The integration of tactile information with electrode actuation enables smart MEA interfaces that can dynamically adjust to specific patient needs and provide an improvement over electrode-only designs. Work is under way to integrate these devices with current neural prostheses for *in-vivo* experiments.

ACKNOWLEDGEMENTS

This work was funded in part by Engineering Research Centers Program of the NSF under Award Number EEC-0310723 and the Bill and Melinda Gates Foundation.

REFERENCES

[1] T.W. Berger and D.L.Glanzman, *Toward Replacement Parts for the Brain*: The MIT Press, 2005.

[2] D.C. Rodger et al., "Flexible Parylene-based Microelectrode Technology for Intraocular Retinal Prostheses," in *Proc. NEMS '06*, pp. 743-746.

[3] J.D. Weiland, W. Liu, and M.S. Humayun, "RETINAL PROSTHESIS," *Ann. Rev. of Bio. Eng*, vol. 7, pp. 361-401, 2005.

[4] Z. Wang and Y. Xu, "Theoretical and Experimental Study of Annular-Plate Self-Sealing Structures," *JMEMS* vol. 17, pp. 185-192, 2008.

[5] H. Zhang et al. "Study and Applications of a Parylene Self-Sealing Structure," in *Proc. MEMS 2006*, pp. 282-285.

[6] S. Timoshenko and S. Woinowsky-Kreiger, *Theory of Plates and Shells*, 2nd ed. New York: McGraw-Hill, 1959.

[7] G. Wollensak and E. Spoerl, "Biomechanical Characteristics of Retina," *Retina, J. Ret. and Vit. Dis.* vol. 24, 2004.

[8] M.E. Hammer, W.H. Peters, and W. Wu, "Basic Mechanical Properties of Retina in Simple Elongation," *J. Bio. Eng.*, vol. 109, 1987.

[9] S. Yang and T. Saif, "Reversible and repeatable linear local cell force response under large stresses," *Exp. Cell Research*, vol. 305, 2005.

CONTACT

* C.A. Gutierrez, tel: 213-821-3949; cagutier@usc.edu